

Dynamics of individual flexible polymers in a shear flow

Philip LeDuc*, Charbel Haber†, Gang Bao* & Denis Wirtz‡

* Department of Mechanical Engineering, † Department of Chemical Engineering, ‡ Department of Materials Science and Engineering, The Johns Hopkins University, Baltimore, Maryland 21218, USA

Polymer dynamics are of central importance in materials science, mechanical engineering, biology and medicine^{1,2}. The dynamics of macromolecular solutions and melts in shear flow are typically studied using bulk experimental methods such as light and neutron scattering and birefringence^{3,4}. But the effect of shear on the conformation and dynamics of individual polymers is still not well understood^{5–7}. Here we describe observations of the real-time dynamics of individual, flexible polymers (fluorescently labelled DNA molecules^{8–15}) under a shear flow. The sheared polymers exhibit many types of extended conformation with an overall orientation ranging from parallel to perpendicular with respect to the flow direction. For shear rates much smaller than the inverse of the relaxation time of the molecule, the relative populations of these two main types of conformation are controlled by the rate of the shear flow. These results question the adequacy of assumptions made in standard models of polymer dynamics^{5,6}.

To visualize the deformation of individual flexible polymers, we use a dilute solution (20 ng ml⁻¹, much smaller than the overlap concentration of ~0.13 mg ml⁻¹) of DNA from the T2 phage that infects *Escherichia coli* suspended in Tris-EDTA buffer and an oxygen-scavenging system to reduce photobleaching. In these conditions, DNA is a flexible polymer with a contour length of ~56 μm, a persistence length of 0.12 μm, a quiescent radius of gyration of 1.5 μm, and an equilibrium relaxation time of $\tau = 1.0 \pm 0.2$ s (measured via dynamic light scattering). DNA molecules are stained with a dye (YOYO-1, Molecular Probes, Eugene, Oregon) for one hour and then placed on a fixed coverslip¹⁶, which is attached to a computer-controlled sliding stage and centred

under an upright microscope (Fig. 1a). The coverslip and sliding stage form the upper and lower plates of the shear flow-cell. This apparatus generates a uniform, laminar shear flow.

We use an SIT (silicon-intensifier target) camera along with an image processor (Hamamatsu, Bridgewater, New Jersey) to capture two-dimensional images, which are recorded in real-time onto S-VHS video and subsequently analysed using a frame grabber. The plane of the two-dimensional images is parallel to the plane formed by the velocity direction, \mathbf{v} ($v = |\mathbf{v}|$), and the vorticity direction, \mathbf{w} , and thus perpendicular to the velocity gradient, $\nabla\mathbf{v}$ (see Fig. 1b). These images are categorized according to the conformational shape displayed by each individual DNA molecule. The entire system is monitored and controlled through a data acquisition system which produces a closed-loop feedback system providing a spatial resolution of motion smaller than one micrometre. Possible wall effects (long-range hydrodynamic interactions between the polymer and the walls of the flow-cell) on molecular conformation are alleviated by using a gap space of 100 μm, which is much larger than the radius of gyration of the molecules (similar results were obtained for gap widths ranging from 100 to 300 μm). Molecules are monitored at the mid-plane of the flow-cell (wall effects appear only when near the walls), with 1-μm depth of focus. The uniformity of the flow field was checked using 1.94-μm-radius polystyrene fluorescent spheres (Duke Scientific Corp., Palo Alto, California) subjected to

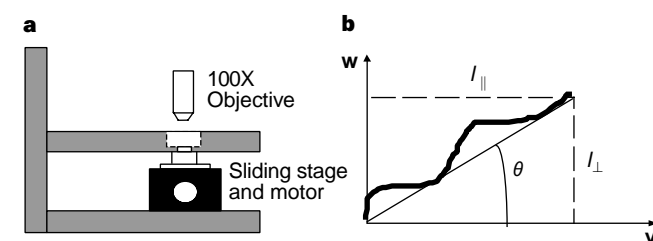
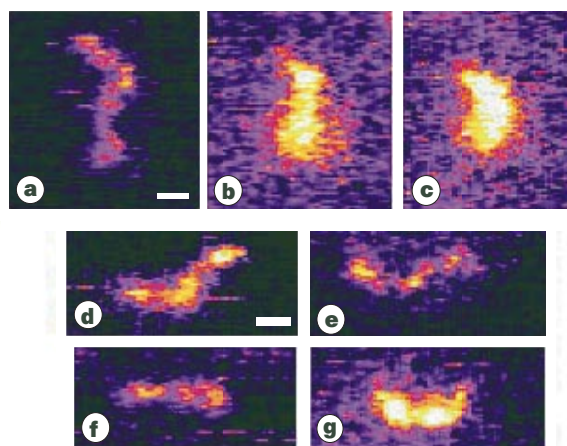
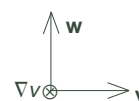


Figure 1 Shear-flow experimental set-up and sketch of an individual DNA molecule. **a**, Diagram of the experimental set-up used to image individual DNA molecules at small strain rates. The top coverslip is immobilized by attaching it to a 2-axis stage. This stage is connected to a Uni-Slide continuous drive system in order to alleviate out-of-plane motion and to a linear variable differential transformer in order to measure the stage displacements. This system is monitored and controlled by a closed-loop computer-controlled system. **b**, For every DNA molecule observed, four quantities are calculated to determine the statistical variation at different strain rates. The contour length is obtained by measuring the total distance along the fluorescent region of the DNA. The parallel and perpendicular lengths are the absolute lengths of the end-to-end segment of the molecule projected onto the axis parallel and perpendicular to the direction of shear flow, respectively. The angle is calculated from the ends of the molecule when compared to the direction of the shear flow. Two-dimensional images of the polymers are recorded in the plane formed by the velocity direction, \mathbf{v} , and the vorticity direction, \mathbf{w} , and thus perpendicular to the velocity gradient, $\nabla\mathbf{v}$, of the shear flow.

Figure 2 The different conformations of DNA under shear. These can be categorized into two main conformational classes: perpendicular or parallel to the flow direction. Although DNA under shear can be loosely categorized into seven subtypes of conformations, **a–g**, we find that these molecules adopt a continuous spectrum of configurations. **a–g**, Images of fluorescently labelled DNA molecules; **a**, conformation characterized by the long thin nature of the DNA and an alignment perpendicular to the flow direction; **b**, conformation characterized by a shorter length and larger width of the DNA than **a**, and alignment in the direction perpendicular to the shear flow; **c**, conformation characterized by the ends of the DNA being in front or behind the main fluorescence region of the DNA molecule, as well as by alignment perpendicular to the direction of shear flow; **d**, conformation characterized by its long thin body and its end-to-end alignment at an angle between 30° and 60° to the direction of the shear flow; **e**, conformation characterized by a long thin body and an alignment parallel to the flow direction; **f**, conformation characterized by a shorter length and larger width of the DNA compared to **e** and its alignment parallel to the direction of the shear flow; **g**, conformation characterized by the ends of the DNA being above or below the main fluorescence region of the DNA molecule and its alignment parallel to the flow direction. Scale bar in **a** is 1 μm and applies to **a–g**. Shear rate is 0.10 s⁻¹.

the same shear flow conditions as the DNA molecules used in the experiments. As expected, the flow generated by the parallel plates is uniform (data not shown)¹⁷.

After systematic observations of individual DNA molecules ($n = 210$) under well defined strain rates, $\dot{\gamma}$, we find that sheared DNA molecules adopt two main types of conformation: either parallel or perpendicular to the flow direction. Relative orientations are calculated from the angle created from the ends of the DNA segments when compared to the direction of flow, and shapes are determined by regions of relative fluorescence intensity along the DNA molecule (Fig. 2; polymers which are out of focus are not considered). Although DNA under shear can be loosely categorized into seven subtypes of conformation (Fig. 2), we find that these molecules adopt a continuous spectrum of configurations. Extended conformations are seemingly absent under no-shear conditions as quiescent DNA molecules display featureless, circular fluorescent regions (data not shown; see also ref. 18).

We observe that a sheared DNA molecule can change both size and orientation dynamically. In Fig. 3a we show a DNA molecule, initially oriented in the direction perpendicular to the flow direc-

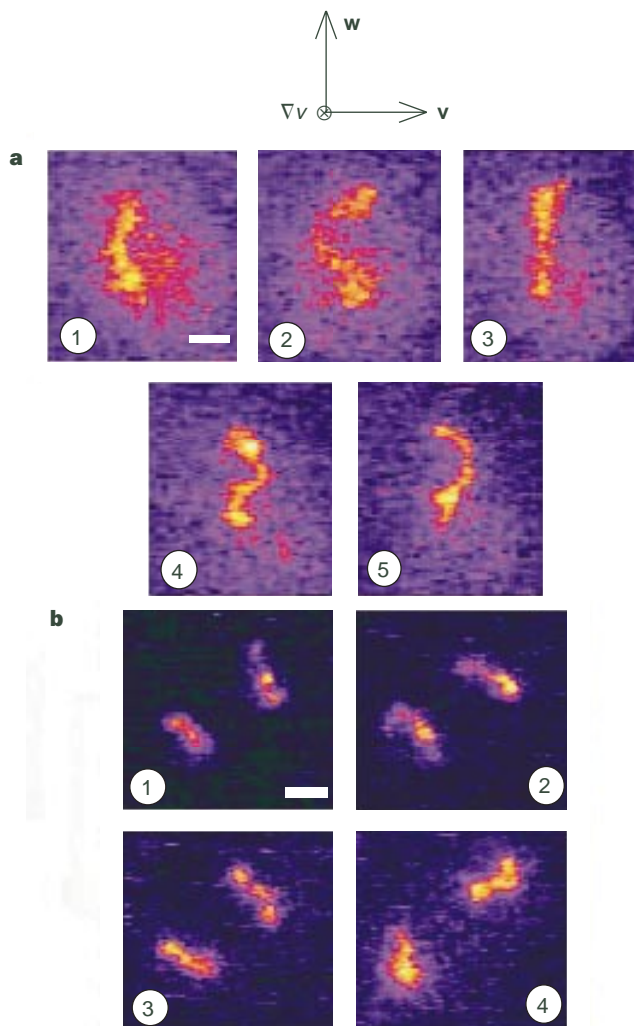


Figure 3 Dynamic motion of DNA molecules experiencing well defined shear strains. **a**, Time-lapse snapshots of a fluorescently labelled DNA molecule subjected to a shear rate of 0.2 s^{-1} . Scale bar in 1 is $1.5 \mu\text{m}$ and applies to 1-5; these numbers indicate the order of the images. The time between images is 2 s. See text for comments. **b**, Time-lapse snapshots of two fluorescently labeled DNA molecules subjected to a shear rate of 0.10 s^{-1} , separated from each other by $\sim 6 \mu\text{m}$. See text for comments. The time between each frame is 2 s. Scale bar in 1 is $2 \mu\text{m}$ and applies to 1-4.

tion, undergoing momentary changes of conformation while maintaining an overall vertical orientation. The extended conformations of sheared DNA molecules typically survive for timescales longer than the relaxation time of an individual molecule in the quiescent state (that is, $>1.0 \text{ s}$). The average time that it takes for a sheared DNA molecule to switch from one of the two main conformational classes (that is, with an overall orientation either parallel or perpendicular to the flow direction) to the other is 4.6 s, 3.9 s, and 3.3 s at shear rates of 0.05 s^{-1} , 0.10 s^{-1} , and 0.20 s^{-1} , respectively. It is remarkable that polymers, which are in close proximity to one another, can undergo dramatically different conformational changes. In Fig. 3b we show two DNA molecules; one changes its conformational changes with $>90^\circ$ rotation.

We further quantified the conformation of individual polymers under shear by computing the instantaneous and time- (or ensemble-) averaged contour length of the DNA molecules, l and $\langle l \rangle$, the length of the projections of the molecule in the directions parallel and perpendicular to the flow direction, l_{\parallel} , $\langle l_{\parallel} \rangle$, l_{\perp} , $\langle l_{\perp} \rangle$, and the angle of the molecule with respect to the flow direction, θ and $\langle \theta \rangle$, respectively (see Fig. 1b for definitions). We find that the instantaneous molecular orientation parameters, l_{\perp} , l_{\parallel} and θ , vary in a seemingly random fashion (Fig. 4). However, in agreement with well-documented bulk measurements of the same quantities, sheared polymers have a tendency to align in the direction parallel to that of the shear flow (Fig. 4). Ensemble-averaged (Fig. 4a and b) and time-averaged (Fig. 4c and d) angles of orientation are $\langle \theta \rangle \approx 0^\circ$ at all tested shear rates. Similarly, $\langle l_{\perp} \rangle$ decreases, and $\langle l_{\parallel} \rangle$ increases, for increasing shear rates (Fig. 4d). The population of the two main conformational classes is influenced by the shear rate of the flow. As

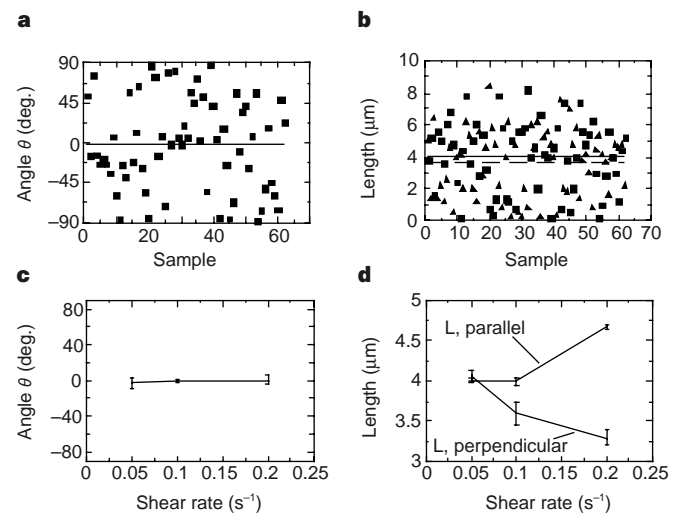


Figure 4 Quantitative characterization of the conformation of individual DNA molecules under shear. **a**, Instantaneous variation (filled squares) and ensemble-averaged value (line) of the angle between sheared polymers and the shear flow direction for a sequential set of samples at the same shear rate. **b**, Instantaneous variation (filled squares, filled triangles) and ensemble-averaged value (line, dashed line) of respectively parallel and perpendicular absolute lengths for a sequential set of images. For **a** and **b**, samples are taken sequentially and monitored while in the field of vision at a shear rate of 0.20 s^{-1} . **c**, Time-averaged angle of orientation of sheared DNA molecules as a function of shear rate. The ensemble-averaged angle of orientation (line) is around zero for all of the shear strain rates tested. **d**, Time-averaged parallel and perpendicular lengths, $\langle l_{\parallel} \rangle$ and $\langle l_{\perp} \rangle$, as a function of shear rate. The relative populations of the two main conformational classes for different shear rates (respectively $0.05, 0.1, 0.2 \text{ s}^{-1}$) are as follows. Vertical conformation (per cent): 42, 35, 23; horizontal conformation (per cent): 36, 44, 58. Percentages are based on the total number of DNA molecules that are in focus and the qualitative categorization by shape and orientation of the molecules. Molecules that are out of the focal plane of the fluorescence microscope are not considered.

the shear rate increases, the DNA molecules tend to align more towards the flow direction (see Fig. 4 legend).

Polymers extended in the direction of the shear flow have been qualitatively predicted by classical theories, and have been indirectly observed by using bulk birefringence^{3,4}. Partial stretching of individual polymers in the direction parallel to the flow direction is due to the viscous drag exerted on the molecule⁵, which has been invoked to explain shear-thinning in polymer solutions¹. However, the existence of vertical conformations (such as those shown in Fig. 2a–c) is unexpected, and is not considered by classical models of polymer physics^{5,6}. Classically, it is assumed that, in the plane parallel to the velocity and the velocity-gradient directions, shear orients polymers at an angle $\leq 45^\circ$ with the flow direction. Shear may also induce tumbling of the polymers within such a plane. However, in the plane parallel to the velocity and the vorticity directions (the present plane of visualization; see Fig. 1), neither shear-induced alignment nor polymer tumbling can explain the existence of vertical conformations. Although fluid-mechanics models—such as Jeffery orbits describing the motion of axisymmetric rigid particles in a shear flow—may serve as limiting-case analyses^{19–23}, they cannot be directly applied to the dynamics of flexible polymers reported here. Furthermore, classical polymer theories predict⁵ that a flexible polymer becomes stretched and oriented when the Weissenberg number, $We = \dot{\gamma}\tau$, is equal to or larger than unity. But here we find shear-induced deformation of flexible polymers can occur at Weissenberg numbers much smaller than unity (Figs 1–4).

Our experimental results show that conventional approaches, such as birefringence and light scattering, which measure only ensemble-averaged molecular parameters (that is, $\langle \theta \rangle$, $\langle l \rangle$), overlook the extremely rich dynamics of individual polymers under shear. Our observations also provide an insight into the conformational and orientational changes of polymers in a shear flow, and a basis for further theoretical modelling. The molecular-level approach to non-equilibrium polymer physics that we describe here could be readily extended to many other polymer systems, including entangled solutions of flexible polymers and semiflexible polymers such as actin^{24,25}. □

Received 21 October 1998; accepted 22 March 1999.

- Munk, P. *Introduction to Macromolecular Science* (Wiley & Sons, New York, 1989).
- Hoffman, A., Ratner, B. & Horbett, T. *Polymers as Biomaterials* (Plenum, New York, 1995).
- Fuller, G. G. *Optical Rheometry of Complex Fluids* (Oxford Univ. Press, New York, 1995).
- Janeschitz-Kriegl, H. *Polymer Melt Rheology and Flow Birefringence* (Springer, New York, 1983).
- Doi, M. & Edwards, S. F. *The Theory of Polymer Dynamics* (Clarendon, Oxford, 1986).
- de Gennes, P. G. *Scaling Concepts in Polymer Physics* (Cornell Univ. Press, Ithaca, 1991).
- de Gennes, P. G. Molecular individualism. *Science* **276**, 199 (1997).
- Matsumoto, M. *et al.* Direct observation of Brownian-motion of macromolecules by fluorescence microscope. *J. Polym. Sci.* **30**, 779–783 (1992).
- Perkins, T. T., Quake, S. R., Douglas, D. E. & Chu, S. Relaxation of a single DNA molecule observed by optical microscopy. *Science* **264**, 822–826 (1994).
- Perkins, T. T., Smith, D. E. & Chu, S. Single polymer dynamics in an elongational flow. *Science* **276**, 2016–2021 (1997).
- Schwartz, D. C. & Koval, M. Conformational dynamics of individual DNA molecules during gel electrophoresis. *Nature* **338**, 520–522 (1989).
- Shivashankar, G. & Libchaber, A. Single DNA molecule grafting and manipulation using a combined atomic force microscope and an optical tweezer. *Appl. Phys. Lett.* **7**, 3727–3729 (1997).
- Smith, D. E., Perkins, T. T. & Chu, S. Dynamical scaling of DNA diffusion coefficients. *Macromolecules* **29**, 1372–1373 (1996).
- Smith, S. B., Finzi, L. & Bustamante, C. Direct mechanical measurements of the elasticity of single DNA molecules by using magnetic beads. *Science* **258**, 1122–1126 (1992).
- Wirtz, D. Direct measurement of the transport properties of a single DNA molecule. *Phys. Rev. Lett.* **75**, 2436–2439 (1995).
- Morikawa, K. & Yanagida, M. Visualization of individual DNA molecules in solution by light microscopy: DAPI staining method. *J. Biochem.* **89**, 693–696 (1981).
- Archer, L. A., Larson, R. G. & Chen, Y. L. Direct measurement of slip in sheared polymer solutions. *J. Fluid Mech.* **301**, 133–151 (1995).
- Matsumoto, S., Morikawa, K. & Yanagida, M. Light microscopic structure of DNA in solution studied by the 4',6-diamidino-2-phenylindole staining method. *J. Mol. Biol.* **152**, 501–516 (1981).
- Jeffery, G. B. The motion of ellipsoidal particles immersed in a viscous fluid. *Proc. R. Soc. Lond. A* **102**, 161–179 (1922).
- Leal, L. G. & Hinch, E. J. The effect of weak Brownian rotations on particles in shear flow. *J. Fluid Mech.* **46**, 685–703 (1971).
- Hinch, E. J. The deformation of a nearly straight thread in a shearing flow with weak Brownian motions. *J. Fluid Mech.* **75**, 765–775 (1976).
- Hinch, E. J. The distortion of a flexible inextensible thread in a shearing flow. *J. Fluid Mech.* **74**, 317–333 (1976).
- Hinch, E. J. Mechanical models of dilute polymer solutions in strong flows. *Phys. Fluids* **20**, S22–S30 (1977).

- Xu, J., Palmer, A. & Wirtz, D. Rheology and microrheology of semiflexible polymer solutions: actin filament networks. *Macromolecules* **31**, 6486–6492 (1998).
- Ostap, E. M., Yanagida, T. & Thomas, D. D. Orientational distribution of spin-labeled actin oriented by flow. *Biophys. J.* **63**, 966–975 (1992).

Acknowledgements. We thank M. Ferro, L. Archer, J. Harden, D. Lavan, and J. van Zanten for discussions. This work was supported by NASA (D.W.), ACS-PRF (D.W.), NSF (D.W.), the Whitaker Foundation (D.W.), Merck, Inc. (D.W.) ARO (G.B.), and IMRE (G.B.)

Correspondence and requests for materials should be addressed to D.W. (e-mail: wirtz@jhu.edu).

Tuning bilayer twist using chiral counterions

R. Oda*†, I. Huc*, M. Schmutz‡, S. J. Candau† & F. C. MacKintosh§†

* Institut Européen de Chimie et Biologie, ENSCPB Av. Pey Berland, BP 108, 33402 Talence Cedex, France

† Laboratoire de Dynamique des Fluides Complexes, 3 Rue de l'Université, 67000 Strasbourg, France

‡ Institut de Génétique et de Biologie Moléculaire et Cellulaire, INSERM/CNRS/ULP, BP 163, 67404 Illkirch Cedex, France

§ Department of Physics, University of Michigan, Ann Arbor, Michigan 48109-1120, USA

From seashells to DNA, chirality is expressed at every level of biological structures. In self-assembled structures it may emerge cooperatively from chirality at the molecular scale. Amphiphilic molecules, for example, can form a variety of aggregates and mesophases that express the chirality of their constituent molecules at a supramolecular scale of micrometres (refs 1–3). Quantitative prediction of the large-scale chirality based on that at the molecular scale remains a largely unsolved problem. Furthermore, experimental control over the expression of chirality at the supramolecular level is difficult to achieve^{4–7}: mixing of different enantiomers usually results in phase separation¹⁸. Here we present an experimental and theoretical description of a system in which chirality can be varied continuously and controllably ('tuned') in micrometre-scale structures. We observe the formation of twisted ribbons consisting of bilayers of gemini surfactants (two surfactant molecules covalently linked at their charged head groups). We find that the degree of twist and the pitch of the ribbons can be tuned by the introduction of opposite-handed chiral counterions in various proportions. This degree of control might be of practical value; for example, in the use of the helical structures as templates for helical crystallization of macromolecules^{8,9}.

Gemini surfactants, consisting of two identical (twin) surfactants joined by a hydrocarbon spacer of variable length, have been shown to have properties that are unusual compared to those of simple surfactants and lipids¹⁰. Cationic gemini surfactants having chiral counterions such as L-tartrate (Fig. 1) form gels in both water and some organic solvents¹¹ by creating extended networks of the multilamellar twisted ribbons reported here (Fig. 2, helix B). A feature of this system is that the chirality comes from the counterion rather than from the amphiphile itself, which allows us to both adjust the pitch and to introduce excess chirality in the form of sodium tartrate salts.

Similar structures to those that we observe are found for diacetylenic lipids, bile and glutamates^{1,2}, which form long helical strips of membranes with exposed edges (Fig. 2, helix A). However, these helical ribbons are unstable: they evolve into tubules (Fig. 2) consisting of a bilayer (or multilayer) membrane of amphiphilic molecules wrapped in a cylinder which exhibits a 'barber's-pole' pattern on its surface as evidence of its chiral origin.

The twisted ribbons that we observe have several original features. Geometrically, their saddle-like curvature differs from the cylind-